Bull Environ Contam Toxicol (2012) 88:788–792
DOI 10.1007/s00128-012-0583-1

Study on Evaporation Characteristics of a Sessile Drop of Sulfur Mustard on Glass

Hyunsook Jung · Sung Min Myung · Myung Kyu Park · Hae Wan Lee · Sam Gon Ryu

Received: 30 November 2011 / Accepted: 23 February 2012 / Published online: 13 March 2012

Abstract The evaporation characteristics (evaporation rates and process) of a sessile drop of sulfur mustard on glass has been studied using a laboratory-sized wind tunnel, gas chromatograph mass spectrometry, and drop shape analysis. It showed that the evaporation rates of the droplet increased with temperature and air flow. The effect of temperature on the rates was more pronounced at lower air flow. Air flow was less effective at lower temperature. The contact angle of the droplet was initially observed as $\theta = 19.5° \pm 0.7$ and decreased linearly with time until it switched to a constant mode.

Keywords Evaporation · Sulfur mustard · Wind tunnel · Chemical agents

Sulfur mustard (bis(2-chloroethyl)sulfide, abbreviated HD) is a blister chemical agent to form blisters on exposed skin (Yang et al. 1992). It was used in the First World War as a chemical weapon. In addition, abandoned HD bombs had been found in China during the Second World War (Tang et al. 2006). Although sulfur mustard is regulated under the 1993 Chemical Weapons Convention (CWC), it is still possible for terrorists or military organization to use sulfur mustard as a chemical weapon. Furthermore, recent chemical terrorism by AUM Shinrikyo in Japan in 1995 has increased awareness of threats of possible use of chemical agents in public.

H. Jung (✉) · S. M. Myung · M. K. Park · H. W. Lee · S. G. Ryu
Agency for Defense Development, Yuseong-Gu, PO Box 35-5, Daejeon 305-600, Korea
e-mail: junghs@add.re.kr

Environmentally, sulfur mustard (HD) persists for 4 years after it is deposited in soil (Brevett et al. 2007). The possible fates of agents upon deposition are adsorption, evaporation, or degradation (Brevett et al. 2009). Contrary to many reports on adsorption and degradation of sulfur mustard (Tang et al. 2006, 2009), there is very little known in open literature regarding the evaporation of HD since the experiment of evaporation of the toxic chemicals can produce a considerable environmental risk and pose a hazard in human body.

We employed a laboratory-sized wind tunnel which allows the reliable measurements of evaporation rates of the hazardous droplet for varying temperature, air flow, humidity, and substrates in a controlled environment (Weber et al. 2006). Although the evaporation is affected by multiple factors such as volatility of the chemical itself, temperature, wind speed, humidity, drop size, substrate properties, and chemical or physical reaction (Westin et al. 1998), we focused the effect of temperature and air flow on the initial evaporation rates of HD droplet on glass. We employed gas chromatography–mass spectrometry method (GC/MS) to analyze the released vapors of HD droplet from wind tunnel during evaporation which were timely collected using thermal desorption tubes. We also performed the measurement of the change in contact angle of HD droplet on glass with time to investigate the evaporation process.

Materials and Methods

Sulfur mustard (HD) has purity >95% by GC–MS analysis (Caution: HD is a highly toxic chemical and should be handled only by trained personnel using applicable safety procedures). Prior to the experiments of wind tunnel, the

glass slides (a 38 mm diameter circle) were washed in a laboratory detergent, rinsed extensively with deionized water, hexane, and ethanol, and dried with a Kimwipe®. The use of wind tunnel has been well described in the literature (Weber et al. 2006; Brevett et al. 2008). In brief, the glass slide with 6-μL drop (corresponding to 1.1–1.3 mg/μL) of HD on it was placed on the piston and inserted into wind tunnel where temperature and air flow was controlled by a Miller-Nelson environmental control unit (Monterey, CA). A variety of temperature (15, 25, 35, and 50°C) and air flow (175 and 375 standard liters per minute (SLPM), corresponding to the measured velocity values at a 2-cm height of 1.79, and 3.70 m/s, respectively) was applied. The flow volume was 100 mL/min.

The vapors from HD droplet on glass were collected on thermal desorption tubes (Markes Tenax) at the vapor sampling inlet. The tubes were automatically switched using a tube sampler every 5–30 min for 7–8 h. HD vapor adsorbed on each tube was desorbed from the thermal desorption tubes using a Markes UNITY/ULTRA Desorption system (Markes International, Liantrisant, UK) and analyzed using an Agilent 7890/5973 GC/MS equipped with HP-5MS capillary column (30 m long, 0.25 mm id, 0.25 μm film thickness). In the thermal desorption system, each sample was pre-purged for 1 min and then desorbed for 10 min at 250°C. The transfer line to the GC was heated to 120°C. The GC oven temperature profile was ramped from 60°C (1 min) to 280°C (2 min) at 40°C/min. The column flow rate (at 60°C) was 1.2 mL/min at a constant pressure of 10.3 psi. The injection temperature was 250°C, MSD transfer line 280°C, MSD quad 150°C, and MSD source at 230°C. The sample extracts were analyzed in the electron impact (EI) mode scanning from 35 to 300 amu with 5.19 scans/s. Under these conditions, HD was eluted at t = 4.6 min (Fig. 1a). The molecular ion for HD (m/z = 158) and the characteristic fragment ion at 109 were seen in MS (Fig. 1b). The agent concentration (mg/m^3) and initial evaporation rates (μg/min) were calculated from the known sample volume and wind tunnel air flow.

The evaporation profiles were generated by dividing the amount of HD collected (mg) over a period of time by the volume of air that had passed through the thermal desorption tube during that period time (in m^3) to give a HD vapor concentration in the air in milligrams per cubic meter (mg/m^3). An additional representation of the data was derived by computing the HD remaining (mg) by subtracting the amount of agent on the tube from the initially measured HD droplet mass. This produced a curve of HD remaining (mg) versus time and the slope for the curve was then computed during the linear portion in order to obtain the initial evaporation rate ($r^2 = 0.999$). All data were averaged from the triplicate independent measurements (SD = ±1.7). We also monitored the disappearance of HD droplet on glass slide using a monitor type borescope (AU559M, DT, Taiwan) which was set at the top ceiling of the inside wind tunnel.

In a separate experiment, we performed the measurements of dynamic contact angles for HD droplet on glass using a drop shape analysis (DSA100, KRÜSS). A 1-μL drop of HD on glass was dispensed onto glass slide through a syringe needle. The advancing and receding contact angles were measured with a circle fit using DSA1 (v1.92) fitting software. Three to five experiments were conducted on different areas of each sample with the averaged contact angles typically varying by ±0.7°.

Results and Discussion

In a first experiment, we studied the initial evaporation rate of HD droplet for varying temperature and air flow. It was obtained by measuring the evaporated HD concentration on glass substrate within the wind tunnel at a series of times. Figure 2 shows the representative evaporation profiles of HD droplet on glass at various temperature and air flow. The temperature increased from 15, 25, and 35 to 50°C with the air flow of 175 and 375 SLPM, respectively. The evaporation of HD droplet on glass was measured until no further decrease in HD vapor concentration was detected by GC/MS. The amount of HD vapor was quantified based upon a standard calibration curve and summation of the concentrations over time yielded the cumulative amount of HD evaporated from glass. In fact, the initial evaporation rates of HD increased proportionally with increasing temperature and air flow. For instance, it was obtained that 9 (at 15°C), 16 (at 25°C), 29 (at 35°C), and 57 μg/min (at 50°C) with air flow of 175 SLPM and 35 (at 25°C), 45 (at 35°C), and 114 (at 50°C) μg/min with air flow of 375 SLPM, respectively. In particular, the effect of temperature on the initial evaporation rates of HD on glass is more pronounced at lower air flow than at higher air flow (Fig. 2b). This indicates that temperature could be a significantly important factor when the air flow is not considerably fast. On the other hand, air flow was less effective at lower temperature (Fig. 2e). In fact, the initial evaporation rate of HD droplets was more or less similar at 25 and 35°C at 175 and 375 SLPM. However, the initial evaporation rate of HD was significantly enhanced at 50°C with air flow of 375 SLPM where the maximum initial evaporation rate was observed (Fig. 2e). It also suggests that air flow could significantly contribute to the initial evaporation rates of HD droplet on glass at extremely higher temperature.

Figure 3 shows the photographs of a 6-μL drop of HD placed onto glass at the variety of temperature with air

flow of 175 SLPM. The drop initially occupied only a 2–3 mm diameter. The HD continuously evaporated from the upper side of the droplet and with time the droplet has begun to visibly fade, indicating a loss of agent at the surface. As shown in Fig. 3, the time length of the drop loss was shortened with increasing temperature with the same air flow. In fact, taking photographs of HD droplet became difficult to detect after the droplet was flattened.

In a separate experiment, we measured the change of contact angle of HD droplet (1 μL) with time to monitor the evaporation process of HD droplet on glass. The experiment was made at room temperature with no control of air flow. The initial contact angle of HD droplet on glass was obtained as $\theta = 19.5° \pm 0.7$. Compared to the reported value ($\theta \sim 28°$), the contact angle of HD on glass is lower. It could be attributed to the different way of cleaning. The change of contact angle of HD droplet with time was shown in Fig. 4a. The contact angle of HD droplet on glass decreased continuously until about 70 min, and then switched to a constant angle mode. The profile of contact angle with time is strongly reminiscent of the evaporation profile of HD droplet shown in Fig. 2. However, we could not directly correlate it with wind tunnel data. On the other hands, the select images shown in Fig. 4b clearly indicate the evaporation process of HD droplet on glass, specifically after the droplet was flattened. In fact, the evaporation of HD droplet begins with constant contact area mechanism (reducing contact angle), and then changes to a constant contact angle mechanism. In other words, the HD droplet begins to shrink its surface area on glass after the upper side of the droplet is all evaporated. These results are also in a good agreement with the report by Navaz et al. (2008).

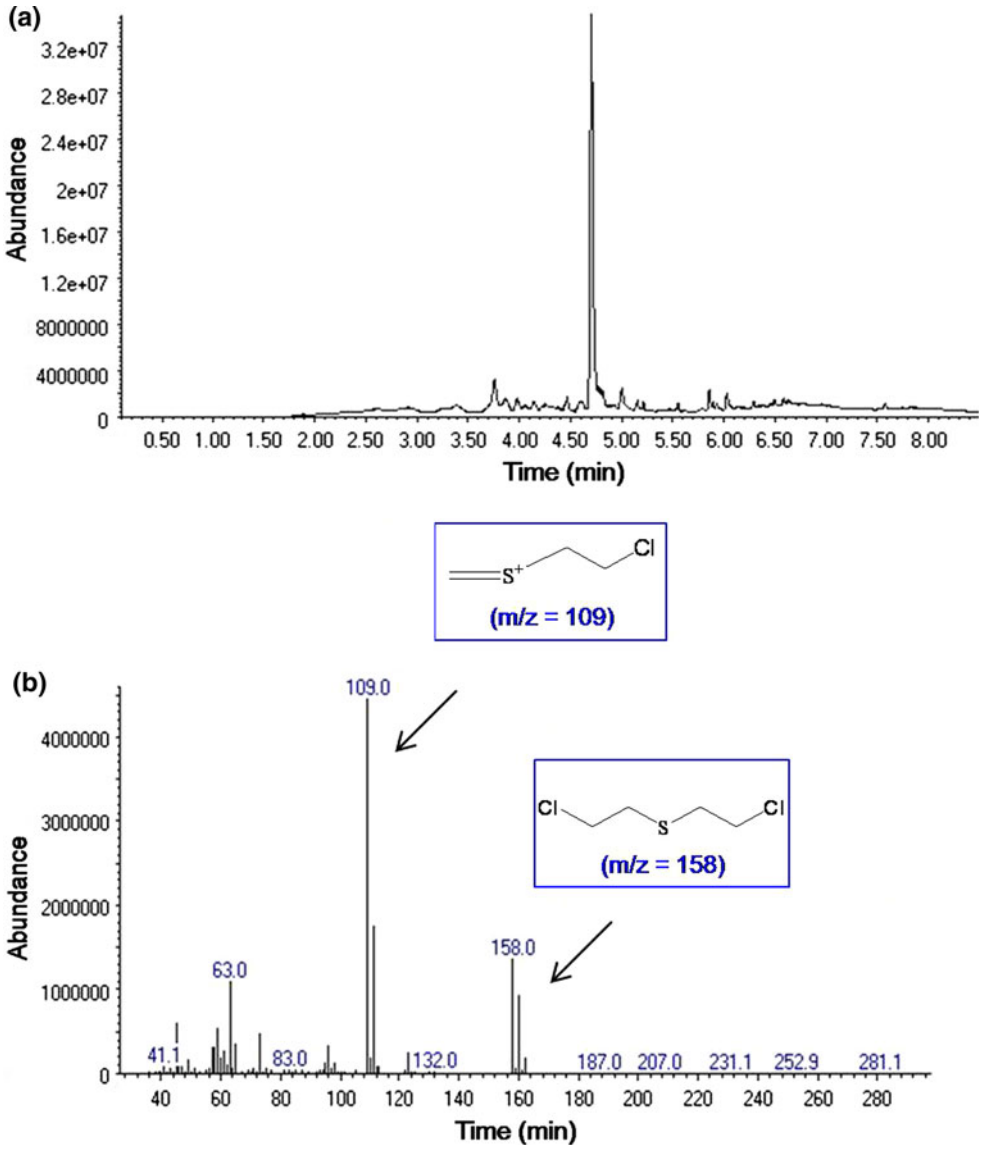

Fig. 1 Spectra of GC/MS of HD vapor. **a** GC of HD of retention times at 4.6 min. **b** MS of the 4.6 min HD peak and the major characteristic ions seen are m/z = 109 and 158

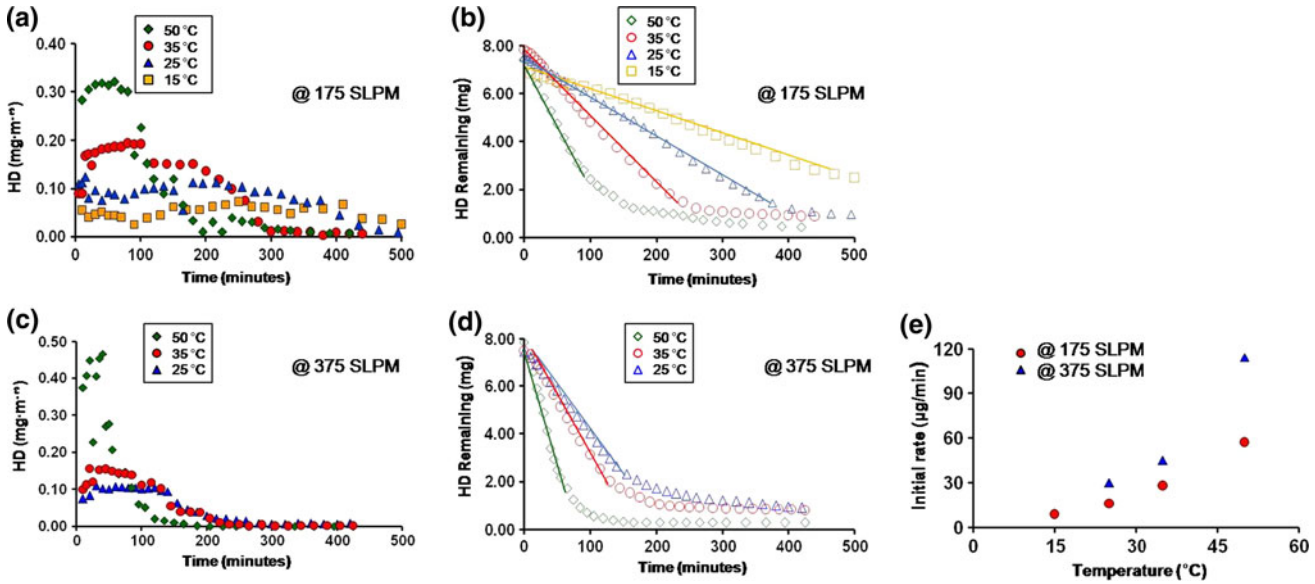

Fig. 2 Representative evaporation profiles at various conditions. **a** and **c** HD vapor concentration (mg/m^3) versus time. **b** and **d** HD remaining (mg) versus time at different temperature with the constant air flow of 175 and 375 SLPM, respectively. The linear portions (solid line, each) of graphs in **b** and **d** were used to calculate the initial evaporation rates. **e** Plot of initial evaporation rates versus temperature and air flow. Data shown in (**e**) are averaged from three independent experiments (SD = ±1.7)

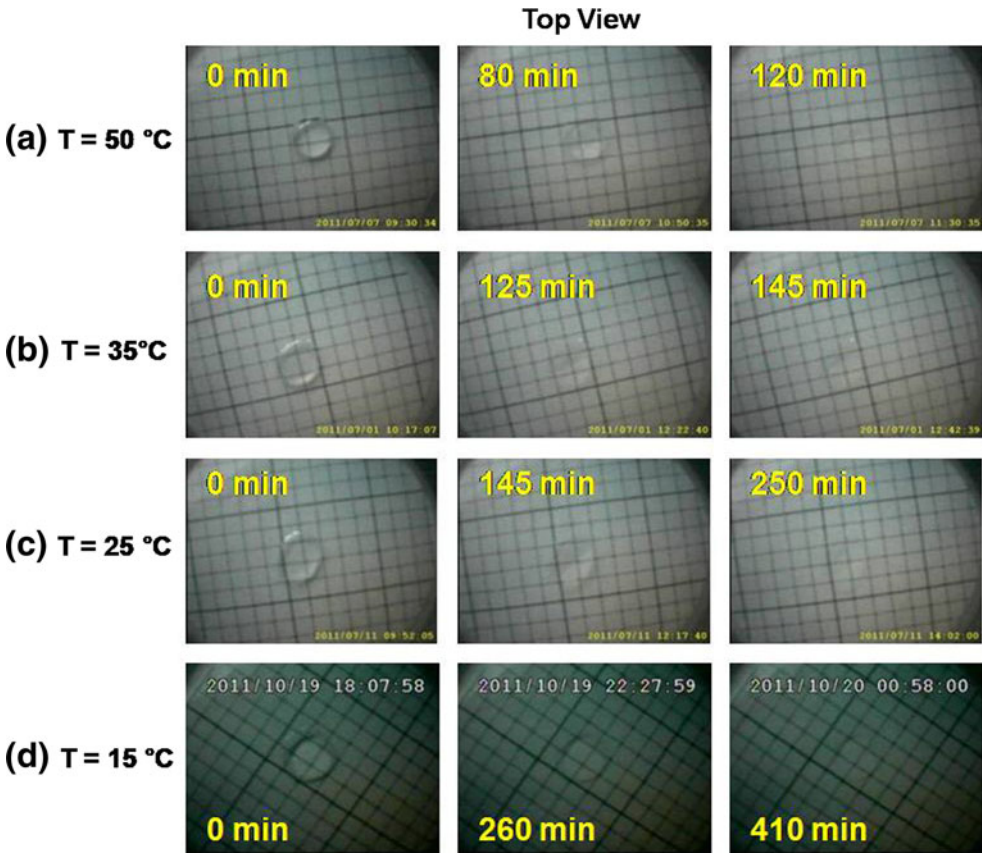

Fig. 3 Photographs of HD droplet on glass within wind tunnel during evaporation: **a** at T = 50°C, **b** at T = 35°C, **c** at T = 25°C, and **d** at T = 15°C. Air flow was kept constant as 175 SLPM for all temperature. The monitor type borescope was fixed at ceiling of wind tunnel in order to take pictures of the upper side of the droplet. A section paper was inserted under the glass for visualization. Graduations in paper are 1.2 mm apart

Summarizing the obtained results it can be stated that the initial evaporation rates of HD on glass substrate were significantly affected by temperature and air flow. In addition, the evaporation of HD droplet on glass proceeds by the two mechanisms: it begins with the constant surface area mechanism and then switches to the constant contact

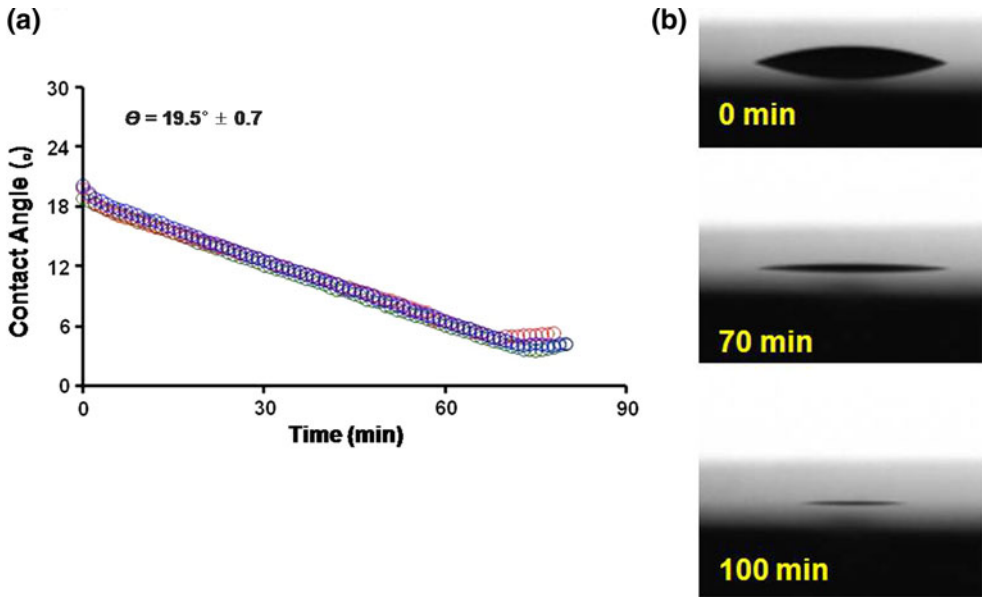

Fig. 4 **a** Evolution of contact angles for HD drop of volume 1 μL on glass surface. Three independent experimental data were shown in **a**. **b** Select images of HD droplet on glass obtained during the measurement of contact angle with time

angle mechanism. Although further study is essential, particularly on other substrates such as soil, concrete, etc., our results are not only important in military aspects but are also applicable to pesticides or other toxic industrial chemicals which are rarely studied due to their toxicity. Furthermore, they can be utilized to develop chemical hazard prediction model that predicts vapor and contact hazard persistence in the air and on surfaces.

Acknowledgments The authors are indebted to Chemical Analysis Test and Research Lab for providing sulfur mustard and Dr. Byun for encouragement to accomplish this project.

References

Brevett CAS, Sumpter KB, Wagner GW, Rice JS (2007) Degradation of the blister agent sulfur mustard, bis(2-chloroethyl)sulfide, on concrete. J Hazard Mater 140:353–360

Brevett CAS, Pence JJ, Nickol RG, Myers JP, Maloney EL, Giannaras CV, Flowers A, Sumpter KB, Durst HD, King BE (2008) Evaporation rates of chemical warfare agents using 5-cm wind tunnels, I. Casarm sulfur mustard (HD) from glass. Edgewood Chemical Biological Center, Technical Report ECBC-TR-647

Brevett CAS, Sumpter KB, Pence J, Nickol RG, King BE, Giannaras CV, Durst HD (2009) Evaporation and degradation of VX on silica sand. J Phys Chem C 113:6622–6633

Navaz HK, Chan E, Markicevic B (2008) Convective evaporation model of sessile droplets in a turbulent flow-comparison with wind tunnel data. Int J Therm Sci 47:963–971

Tang H, Cheng Z, Xu M, Huang S, Zhou L (2006) A preliminary study on sorption, diffusion, and degradation of mustard (HD) in cement. J Hazard Mater B128:227–232

Tang H, Cheng Z, Zhou L, Zuo G, Kong L (2009) Degradation of sulfur mustard and sarin over hardened cement paste. Environ Sci Technol 43:1553–1558

Weber DJ, Scudder MK, Moury CS, Shuely WJ, Molnar JW, Miller MC (2006) Development of the 5-cm agent fate wind tunnel. Edgewood Chemical Biological Center, Technical Report ECBC-TR-327, AD-A462 884

Westin SN, Winter S, Karlsson E, Hin A, Oeseburg F (1998) On modeling of the evaporation of chemical warfare agents on the ground. J Hazard Mater A 63:5–24

Yang YC, Baker JA, Ward JR (1992) Decontamination of chemical warfare agents. Chem Rev 92:1729–1743